



NIH Public Access

Author Manuscript

Cancer Res. Author manuscript; available in PMC 2012 September 15.

Published in final edited form as:

Cancer Res. 2012 March 15; 72(6): 1494–1503. doi:10.1158/0008-5472.CAN-11-3948.

ARN-509: a novel anti-androgen for prostate cancer treatment

Nicola J. Clegg¹, John Wongvipat^{1,2}, Jim Joseph¹⁰, Chris Tran¹, Samedy Ouk⁹, Anna Dilhas³, Yu Chen^{1,8}, Kate Grillot¹⁰, Eric D. Bischoff¹⁰, Ling Cai¹, Anna Aparicio¹⁰, Steven Dorow, Vivek Arora^{1,8}, Gang Shao¹⁰, Jing Qian¹⁰, Hong Zhao³, Guangbin Yang³, Chunyan Cao³, John Sensintaffar¹⁰, Teresa Wasielewska¹, Mark R. Herbert¹⁰, Celine Bonnefous¹⁰, Beatrice Darimont¹⁰, Howard I. Scher⁸, Peter Smith-Jones⁴, Mark Klang⁵, Nicholas D. Smith¹⁰, Elisa De Stanchina⁶, Nian Wu⁷, Ouathek Ouerfelli³, Peter J. Rix¹⁰, Richard A. Heyman¹⁰, Michael E. Jung⁹, Charles L. Sawyers^{1,2}, and Jeffrey H. Hager¹⁰

¹Human Oncology & Pathogenesis Program, Department of Medicine, Memorial Sloan-Kettering Cancer Center, New York, NY 10065

²Howard Hughes Medical Institute, Department of Medicine, Memorial Sloan-Kettering Cancer Center, New York, NY 10065

³Organic Synthesis Core Facility, Department of Medicine, Memorial Sloan-Kettering Cancer Center, New York, NY 10065

⁴Molecular Pharmacology & Chemistry, Department of Medicine, Memorial Sloan-Kettering Cancer Center, New York, NY 10065

⁵Research Pharmacy Core Facility, Department of Medicine, Memorial Sloan-Kettering Cancer Center, New York, NY 10065

⁶Antitumor Assessment Core Facility, Department of Medicine, Memorial Sloan-Kettering Cancer Center, New York, NY 10065

⁷Analytical Pharmacology Core Facility, Department of Medicine, Memorial Sloan-Kettering Cancer Center, New York, NY 10065

⁸Genitourinary Oncology Service, Department of Medicine, Memorial Sloan-Kettering Cancer Center, New York, NY 10065

⁹Department of Chemistry and Biochemistry, University of California, Los Angeles, CA 90095

¹⁰Aragon Pharmaceuticals, Inc., San Diego, CA 92130

Abstract

Continued reliance on the androgen receptor (AR) is now understood as a core mechanism in castration-resistant prostate cancer (CRPC), the most advanced form of this disease. While established and novel AR-pathway targeting agents display clinical efficacy in metastatic CRPC, dose-limiting side effects remain problematic for all current agents. In this study, we report the discovery and development of ARN-509, a competitive AR inhibitor this is fully antagonistic to AR overexpression, a common and important feature of CRPC. ARN-509 was optimized for inhibition of AR transcriptional activity and prostate cancer cell proliferation, pharmacokinetics

Correspondence: Charles L Sawyers: Human Oncology & Pathogenesis Program & Howard Hughes Medical Institute, Memorial Sloan-Kettering Cancer Center, 1275 York Avenue Box 20, New York, NY 10065, USA; Tel 646-888-2594; Fax 646-888-2595, sawyersc@mskcc.org. Jeffrey H Hager; Aragon Pharmaceuticals, 12780 El Camino Real, Suite 301, San Diego, CA 92130, Tel 858-369-7608; Fax:858-369-7656, jhager@aragonpharm.com.

Potential conflicts of interest: Patent applications: JW, CT, SO, MJ, CLS are co-inventors of ARN-509 and MDV3100; AD, OO, HZ, GY are co-inventors of an ARN-509 synthetic method. CLS, MEJ are consultants to Aragon and own Aragon stock. JJ, KG, EDB, AA, GS, JQ, JS, MRH, CB, BD, NDS, PJR, RAH, JHH are Aragon employees and own Aragon stock. NJC owns Aragon stock.

and *in vivo* efficacy. In contrast to bicalutamide, ARN-509 lacked significant agonist activity in preclinical models of CRPC. Moreover, ARN-509 lacked inducing activity for AR nuclear localization or DNA binding. In a clinically valid murine xenograft model of human CRPC, ARN-509 showed greater efficacy than MDV3100. Maximal therapeutic response in this model was achieved at 30 mg/kg/day of ARN-509, whereas the same response required 100 mg/kg/day of MDV3100 and higher steady-state plasma concentrations. Thus, ARN-509 exhibits characteristics predicting a higher therapeutic index with a greater potential to reach maximally efficacious doses in man than current AR antagonists. Our findings offer preclinical proof of principle for ARN-509 as a promising therapeutic in both castration-sensitive and castration-resistant forms of prostate cancer.

Keywords

prostate cancer; castration-resistant prostate cancer; anti-androgen; androgen receptor

Introduction

Castration-resistant prostate cancer (CRPC) is the second-most common cause of cancer-related deaths in American men (32,000 deaths/year) (1). Treatment of localized tumors is often curative; however, metastatic disease emerges in ~25% of patients (2). The disease is initially sensitive to androgen-deprivation therapies (castration-sensitive disease state), but resistance is inevitably acquired, leading to CRPC which is incurable. Despite administration of androgen-depleting therapies, continued androgen receptor (AR) signaling is a common feature of CRPC, attributed to AR gene-amplification, AR gene mutation, increased AR expression or increased androgen biosynthesis in prostate tumors (2). Bicalutamide, a clinically-used anti-androgen, competes with androgens for binding AR; however, in the setting of CRPC, bicalutamide undergoes an antagonist-to-agonist switch, stimulating AR activity (measured by increased prostate specific antigen (PSA), an AR-regulated target-gene product) and prostate tumor-cell growth. The continued reliance of CRPC on AR signaling offers opportunities to develop next-generation anti-hormonal agents to treat this disease.

Recently, two agents targeting the androgen-signaling-axis have undergone late-stage clinical-testing for treatment of men with CRPC (3). Abiraterone acetate targets 7- α -hydroxylase/17,20-lyase (CYP17A), thereby inhibiting residual androgen biosynthesis (4, 5), while MDV3100 is an anti-androgen discovered by the Sawyers/Jung groups in a screen for potent anti-androgens lacking agonist activity in context of AR over-expression (6, 7). In a Phase III study, abiraterone acetate (plus the corticosteroid, prednisone) increased overall survival by 3.9 months over control (prednisone only) in CRPC patients previously treated with docetaxel (8). Co-administration of low-dose prednisone is necessary to ameliorate hypertension, hypokalemia and fluid overload resulting from mineralocorticoid excess induced by CYP17-inhibition (8). Whereas co-administration of prednisone is manageable in metastatic CRPC patients, longer-term use in earlier disease phases could be problematic due to potential side effects (diabetes, weight gain, Cushing syndrome and osteoporosis). In Phase I/II studies of MDV3100, significant serum-PSA responses (>50% decrease) were observed in >50% of chemotherapy-naïve and -treated CRPC patients. MDV3100 belongs to a class of anti-androgens that carry seizure risk, likely mediated *via* antagonism of the CNS-based GABA_A receptor (9). MDV3100 dosing-regimens must achieve exposures at steady-state sufficient to drive therapeutic response without exceeding the threshold for adverse effects. Anti-androgens with a high therapeutic-index can be expected to result in safer, more effective treatments across all stages of prostate cancer.

We describe the discovery and preclinical development of ARN-509, an anti-androgen with similar *in vitro* activity to MDV3100 but with greater *in vivo* activity in CRPC xenograft models (6). ARN-509 exhibits anti-tumor activity in a castration-sensitive xenograft model of prostate cancer and anti-androgenic effects in dogs that phenocopy castration. ARN-509, like MDV3100 and other anti-androgens, binds weakly to GABA_A receptors and could potentially cause seizure at high-dose. However, mouse steady-state plasma- and brain-levels are lower for ARN-509 versus MDV3100 at therapeutic doses, suggesting lower seizure-inducing potential for ARN-509. These data support clinical development of ARN-509 for treatment of castration-sensitive and -resistant prostate cancer.

Materials and Methods

Detailed information is presented in Supplemental Materials and Methods. Ligand-binding studies were performed either in a whole-cell assay (LNCaP/AR(cs)), using whole-cell extracts (MDA-MB-453), or *in vitro* with purified receptor. Proliferation assays (VCaP) were performed in either agonist- or antagonist-mode (without/with R1881). RNA was isolated from LNCaP/AR cells for RT-PCR analysis with primers (Suppl. Table 1) specific for AR target-genes. Fluorescence microscopy was performed in LNCaP cells transfected with AR-EYFP as previously described (6). AR antibody PG-21 (Upstate) was used for chromatin immunoprecipitation (ChIP) experiments (LNCaP/AR(cs)) together with primers for PSA (10) and TMPRSS2 (11) enhancers. Luciferase reporter-gene assays were performed in LNCaP/AR-luc or Hep-G2 cells expressing VP16-AR.

Animal studies at MSKCC, Aragon Pharmaceuticals and Covance Laboratories were performed under protocols approved by MSKCC or Aragon Institutional Animal Care and Use Committees and institutional guidelines for humane use of animals in research were followed. *In vivo* xenograft experiments (LNCaP/AR(cs) or LNCaP/AR-luc) and TUNEL- and Ki67-staining were performed as previously described (6). As part of an Investigational New Drug (IND)-enabling toxicity/toxicokinetic study, ARN-509 was administered to male beagle dogs by Covance Laboratories Inc., in accordance with US Food and Drug Administration (FDA) Good Laboratory Practice (GLP) Regulations. Histologic image files are available online (12). Mouse/dog pharmacokinetics were determined by non-compartmental analysis. Tumor- and brain tissue-distribution was quantified by LC-MS/MS. Serum-protein binding was assessed *in vitro* by equilibrium dialysis, using mouse- and human-plasma. GABA_A-binding experiments in membrane-homogenates of rat cerebral cortex used [³⁵S]TBPS competitor with picrotoxinin as a positive-control.

Results

ARN-509 binds AR and inhibits growth and androgen-mediated gene transcription in AR-over-expressing prostate cancer cells

ARN-509 (Fig. 1A) is a synthetic biaryl thiohydantoin compound discovered using structure-activity-relationship (SAR)-guided medicinal chemistry to identify non-steroidal anti-androgens that retain full antagonist-activity in the setting of increased AR expression.

Equilibrium binding-affinity of ARN-509 for AR was measured in competition with 16 β -[¹⁸F]fluoro-5 α -DHT (¹⁸F-FDHT) in a whole-cell binding-assay (LNCaP/AR(cs) cells) (Fig. 1B). ARN-509 (IC₅₀=16 nM) binds AR with 7- to 10-fold greater affinity than the clinically approved anti-androgen, bicalutamide (median IC₅₀=160 nM), and competes for the same binding-site in the ligand-binding pocket of the receptor. Curiously, AR binding-assays using MDA-MB-453 cell-extracts does not differentiate between ARN-509 and bicalutamide, possibly due to cellular-uptake differences in the whole-cell binding-assay (Suppl. Fig. 1). Binding of ARN-509 is selective for AR versus other nuclear hormone

receptors (up to 100 μ M), as shown in competitive binding-assays using *in vitro* purified AR, or estrogen, progesterone or glucocorticoid receptors (ER, PR or GR) (Suppl. Table 2).

Identification of ARN-509 as a lead-candidate for preclinical development was based on initial assessment of both antagonist and agonist activity of AR-signaling in the LNCaP/AR(cs) prostate cancer cell-line. This cell-line was engineered to over-express AR (3–5 fold higher than parental LNCaP), thus mimicking the castration-resistant clinical state (2, 13). In castration-resistant LNCaP/AR cells, ARN-509 (and MDV3100) antagonized androgen-mediated induction or repression of mRNA expression-levels for 13 endogenous genes including PSA and TMPRSS2, whereas bicalutamide was significantly less effective (Fig. 1C). Bicalutamide treatment of LNCaP/AR(cs) cells in absence of the synthetic androgen R1881 resulted in altered gene-expression consistent with its well-documented agonist activity in context of AR over-expression. ARN-509 or MDV3100 did not exhibit agonist activity up to 10 μ M (Fig. 1C). Similar results were obtained with a second, independently derived LNCaP/AR line harboring a stably-integrated AR-regulated probasin:luciferase reporter construct (ARR2-Pb-Luc) (Fig. 2C).

To determine whether inhibition of AR-signaling by ARN-509 is accompanied by reduced tumor-cell proliferation, the number of viable prostate cancer cells was quantified following incubation with anti-androgen. ARN-509 fails to stimulate proliferation of VCaP cells (Fig. 1D, left) and antagonized the proliferative effect of R1881 (Fig. 1D, right), whereas bicalutamide induced cell-proliferation in a dose-dependent manner (Fig. 1D, left), and only partially antagonized the effects of R1881 (Fig. 1D, right). There was no significant effect on growth of AR-negative PC-3 prostate cancer cells, indicating the anti-proliferative effect observed in VCaP cells is mediated through antagonism of AR (Suppl. Fig. 2).

ARN-509 impairs nuclear-localization & DNA-binding in prostate cancer cells

Translocation of AR from cytoplasm to nucleus upon ligand-binding is a highly-regulated essential step in AR-mediated gene-regulation. To determine if ARN-509 impairs AR nuclear-localization and thus reduces the concentration of AR available to bind androgen response-elements (AREs), LNCaP cells expressing AR tagged with enhanced yellow fluorescent protein (AR-EYFP) were treated with DMSO, R1881, bicalutamide or ARN-509. Fluorescence intensities of nuclear (N) and cytoplasmic (C) compartments of individual cells were quantified and the N/C ratio calculated. In DMSO-treated cells, AR-EYFP was largely localized to the cytoplasm (N/C-ratio:0.7), whereas in R1881-treated cells the receptor was localized predominantly in the nucleus (N/C-ratio:29) (Fig. 2A). Bicalutamide treatment also resulted in a significant amount of nuclear AR (N/C-ratio:13.8), although less than that observed with R1881 (6) (Fig. 2A). In contrast, in ARN-509-treated cells much of the AR-EYFP protein remained cytoplasmic (N/C-ratio:2.5) (Fig. 2A). This decrease in nuclear AR was unrelated to turnover or stability, as ARN-509 did not alter steady-state levels of AR as monitored by immunoblot of whole-cell lysates (data not shown).

To explore whether the low levels of nuclear AR following ARN-509 treatment could be recruited to promoters of target genes in prostate cancer-cells with potential to modulate transcription, we carried out chromatin immunoprecipitation (ChIP) experiments in LNCaP/AR cells treated with R1881 and/or anti-androgen. AR was not recruited to the enhancer region of PSA or TMPRSS2 target-genes after ARN-509 or MDV3100 treatment under hormone-depleted conditions (Fig. 2B). In antagonist-mode (co-treatment with R1881 to activate AR), ARN-509 was able to effectively compete with R1881 and prevent AR from binding to promoter-regions (Fig. 2B). In contrast, bicalutamide exhibited partial agonist activity as evidenced by induction of DNA-binding at AR target genes and incomplete antagonism of the effects of R1881 (Fig. 2B).

AR recruitment to DNA promoter-elements and activation of gene-transcription requires interplay of protein cofactors in response to receptor conformational changes upon ligand-binding (14). To remove cofactor-recruitment as a variable that might explain the effects of ARN-509 on AR DNA-binding, we directly assessed the DNA-binding competency of the residual nuclear AR in ARN-509-treated Hep-G2 cells expressing a VP16-AR fusion protein and an ARE-driven luciferase reporter. VP16-AR is constitutively nuclear and drives transcription through AREs in the absence of coactivator protein recruitment, thereby providing a direct assessment of ligand-induced DNA binding (6, 14). In absence of R1881, bicalutamide partially activated VP16-AR-mediated transcription, indicative of AR binding to DNA. In LNCaP/AR-luc cells with a stably integrated AR-driven luciferase reporter construct (6, 14), bicalutamide was unable to activate wtAR (Fig. 2C;upper left panel). In contrast to bicalutamide, ARN-509 did not induce significant VP16-AR-mediated transcription and thus is not competent to induce significant DNA binding at concentrations up to 10 μ M (Fig. 2C;upper right panel). ARN-509 and MDV3100 inhibited R1881-induced VP16-AR-mediated transcription with an IC₅₀ of 0.2 μ M (Fig. 2C). In contrast, in the presence of R1881, bicalutamide showed only weak partial-antagonism of VP16-AR-mediated transcription (IC₅₀ 0.35 μ M;Fig. 2C;lower right panel). This confirms the ChIP findings and underscores the fundamental mechanistic differences between ARN-509 versus bicalutamide.

ARN-509 is a potent inhibitor of tumor growth in murine xenograft models of castration-resistant prostate cancer

ARN-509 exhibits low systemic clearance, high oral bioavailability and long plasma half-life in both mouse and dog, supporting once-daily oral dosing (Suppl. Table 3). Consistent with its long terminal-half-life, ARN-509 steady-state plasma-levels increased in repeat-dose studies, resulting in high C_{24hr} levels and low peak:trough ratios (ratio:2.5; Suppl. Table 4). To assess *in vivo* pharmacodynamic activity of ARN-509 in a model of castration-resistant prostate cancer, castrate male immunodeficient mice harboring LNCaP/AR-luc xenograft tumors (co-expressing exogenous AR and the AR-dependent reporter ARR2-Pb-Luc) were orally treated with either vehicle or ARN-509 (10 mg/kg/day). Following 17 days of treatment, androgen-driven luciferase reporter-gene activity, normalized to tumor volume, was consistently reduced in ARN-509-treated animals compared to vehicle (Fig. 3A), indicating AR inhibition by ARN-509 *in vivo*.

The therapeutic effect of ARN-509 (10 mg/kg/day) was compared to bicalutamide (10 mg/kg/day) in castrate mice bearing LNCaP/AR(cs) xenograft tumors. On day 28, 7/9 vehicle-treated tumors increased in size compared to starting-volume (Fig. 3B, yellow). The anti-tumor activity of bicalutamide in this model was largely restricted to growth-inhibition rather than tumor-shrinkage - only 1/10 tumors exhibited >50% regression (Fig. 3B, green). In contrast, 8/10 ARN-509-treated tumors regressed by >50% (volume), including 2 tumors that were no longer palpable (Fig. 3B, red). Similar results were obtained in castrate male SCID mice bearing LNCaP/AR-luc xenograft tumors (Suppl. Fig 3). Greater efficacy of ARN-509 was achieved despite 3-fold lower steady-state plasma-levels (mean C_{24hr}-concentrations: 9.69 μ g/mL ARN-509 versus 30.74 μ g/mL bicalutamide). Consistent with the potent anti-tumor effect, ARN-509-treated tumors exhibited a 60% decrease in proliferative-index (versus vehicle) and a 10-fold increase in apoptotic rate (versus vehicle) as monitored by Ki-67 staining and TUNEL, respectively (Figs. 3C, D).

To further understand the clinical potential of ARN-509, we compared its antitumor activity to MDV3100 in a series of independent experiments. Castrate male mice bearing LNCaP/AR xenograft tumors were treated with either ARN-509 or MDV3100 at doses of 1, 10 or 30 mg/kg/day. Both compounds showed a dose-responsive effect (Figs. 4A–B) trending towards greater efficacy for ARN-509 versus MDV3100, although none of the pairwise

(equi-dose) comparisons of day 28 tumor-volumes reached statistical significance, due to relatively small cohort-size ($n=7-8$). To define the optimal biological dose (OBD: lowest dose yielding maximum efficacy) for both ARN-509 and MDV3100, tumor-responses in the LNCaP/AR(cs) model were monitored at 30 and 100 mg/kg/day in larger cohorts to increase statistical power ($n=19-20$). Thirteen of 20 ARN-509 (30 mg/kg/day)-treated animals exhibited >50% reduction in tumor-volume at day 28 versus 3 of 19 MDV3100 (30 mg/kg/day)-treated mice (Fig. 4C). A higher MDV3100 dose (100mg/kg/day) resulted in increased efficacy (12/19 tumors with >50% reduction in tumor-volume) compared to the 30 mg/kg/day dose. In contrast, ARN-509 dosed at 100 mg/kg/day (13/19 mice with >50% reduction in tumor-volume) was no more efficacious than 30 mg/kg/day. There was no difference in efficacy between ARN-509 and MDV3100 at 100 mg/kg/day, despite a dose-dependent increase in exposure (ARN-509 and MDV3100 from 30–100 mg/kg) as measured by independent single-dose mouse PK-studies (Suppl. Table 5). These results indicate an OBD in the LNCaP/AR model between 10–30 mg/kg/day for ARN-509, whereas the OBD for MDV3100 lies between 30–100 mg/kg/day.

To define concentrations of ARN-509 necessary to drive therapeutic responses, we measured steady-state plasma and tumor-tissue concentrations following 28 days of continuous dosing of LNCaP/AR(cs) tumor-bearing mice. Steady-state plasma concentrations for ARN-509 were approximately 2–4-fold lower than for an equivalent dose of MDV3100 (Table 1 and Suppl. Table 5), whereas intratumoral levels of ARN-509 and MDV3100 were roughly equivalent, indicating a higher tumor/plasma ratio for ARN-509 (Table 1). A comparative single-dose intravenous PK assessment in mice indicated higher steady state volume-of-distribution (V_{ss}) for ARN-509 (2.1 L/kg) (Suppl. Table 3) versus MDV3100 (0.82 L/kg) (Suppl. Table 6). One determinant of V_{ss} is degree of binding to plasma-proteins. Assessment of *in vitro* free fraction in plasma indicated that ARN-509 is less protein-bound, resulting in a ~2-fold greater free-fraction compared to MDV3100 in mouse and human plasma (Suppl. Table 7).

Recent reports indicate that multiple anti-androgens are also functional antagonists of the GABA_A receptor, implicated to cause seizure in preclinical species and in humans (9). ARN-509 and MDV3100 both exhibit low micromolar affinity (IC_{50} 3.0 and 2.7 μ M, respectively) for the GABA_A receptor in radioligand binding-assays (Suppl. Fig. 4) and thus may potentially antagonize GABA_A at therapeutic dose levels. Degree of permeability of the blood-brain barrier to ARN-509 or MDV3100 is a further determinant of seizure-risk. Steady-state brain-tissue levels of both ARN-509 and MDV3100 (10 mg/kg/day) were measured in mice after 28 days of daily therapy. Unexpectedly, ARN-509 brain-levels were 4-fold lower than those observed with MDV3100 treatment (Table 2), thus suggesting lower seizurogenic potential for ARN-509.

ARN-509 induces castrate-like histopathological changes in androgen-dependent tissues in dogs

Robust anti-androgenic activity in the non-castrate setting would support clinical assessment of ARN-509 in the castration-sensitive phase of prostate cancer. To determine anti-androgenic effects of ARN-509 in context of normal levels of androgen, we assessed effects on androgen-dependent reproductive organs of adult male dogs and on LNCaP/AR xenograft tumor-growth in intact male mice.

ARN-509 dosed at 10 mg/kg/day for 28 days resulted in a 3-fold reduction in weight of dog prostates. Epididymis weight was also reduced (1.7-fold); however, this effect did not reach statistical significance (Fig. 5A). Histopathological analysis of prostates of ARN-509-treated animals showed lack of glandular secretory activity, similar to prostates of sexually immature or castrate animals (Fig. 5B, right-panels).

Anti-androgenic effects on spermatogenesis were evident in ARN-509 treated animals. Epididymides of ARN-509-treated animals exhibited histological changes consistent with anti-androgen-induced atrophy and contained minimal spermatozoa (Fig. 5B, left-panels). Epididymides of vehicle-treated dogs were normal, with abundant spermatozoa (Fig. 5B, left panels).

Cell-proliferation in dog prostate-tissues treated with ARN-509 was significantly lower (reduced Ki67-staining) than in vehicle-treated animals (Fig. 5C). Despite significant atrophy and the well-described increase in prostatic apoptosis following castration (15), there was no change in apoptotic-rate in ARN-509-treated prostates (TUNEL-staining), suggesting that atrophy, if driven by apoptosis, was advanced and complete at 28 days of treatment (Fig. 5C). The epididymides of ARN-509 treated animals exhibited a tendency towards lower proliferative-and higher apoptotic-indices compared with vehicle-treated animals, although Ki67- or TUNEL-positive cells were rare (Suppl. Fig. 5).

Consistent with the anti-androgenic effects observed in the dog, ARN-509 displayed significant anti-tumor activity in LNCaP/AR(cs) xenografts growing in intact (non-castrate) mice (Fig. 5D). At 10 mg/kg/day, the anti-tumor effect of ARN-509 was largely confined to stabilization of tumor-growth. At higher doses of 30 mg/kg/day, robust tumor-regression (>50% reduction in starting tumor volume) was observed in 6/8 ARN-509-treated animals, similar to regressions observed in mice castrated on the day treatment initiated.

Discussion

ARN-509 is a next generation anti-androgen selected for pre-clinical and clinical development based on its efficacy and pharmacodynamic profile in mouse xenograft models of CRPC. Unexpectedly, given a similar in vitro profile, ARN-509 is more efficacious per unit dose- and per unit steady-state plasma-level in mouse models of CRPC than MDV3100. Maximal efficacy at lower steady-state plasma- and brain-levels should result in a higher therapeutic-index and enable dose escalation in man with reduced-risk of seizure and other side-effects. We propose that the ability of ARN-509 to drive efficacy with significantly lower exposures at steady-state is a function of reduced-binding to plasma-proteins, resulting in greater tumor:plasma ratios and more robust antagonism of AR activity. Importantly and unexpectedly, the greater free-fraction of ARN-509 does not result in higher steady-state brain-levels which otherwise could negate any increase in therapeutic index as it relates to GABA_A-antagonism.

The ARN-509 pharmacological effects on male reproductive organs, and anti-tumor activity on LNCaP/AR tumors in intact mice, suggests potential to treat the castration-sensitive disease-phase. In particular, given the improved profile of ARN-509 over bicalutamide, “combined androgen-blockade” (ARN-509 dosed in conjunction with LHRH agonists/antagonists) may be useful in treatment of recurrent disease following primary treatment by surgery or radiation. Given its potential for a high therapeutic-index, ARN-509 is also well-suited to combination therapy with other agents that target key pathways (e.g. PI3K) in prostate tumorigenesis (16).

ARN-509 has completed dose-escalation Phase I study in metastatic CRPC to determine human pharmacokinetics, safety and efficacy (*via* endpoints of PSA response and time-to-PSA progression), and has proceeded into Phase 2 clinical development in distinct subsets of prostate cancer.

Supplementary Material

Refer to Web version on PubMed Central for supplementary material.

Acknowledgments

Plasmids: SP Balk (Beth Israel Deaconess Medical Center), M Diamond (Washington University School of Medicine). Thanks to PA Watson and Sawyers laboratory members for helpful discussions and to FM Sirotnak, LJ McDonald and S Sequira for operational guidance. MSKCC technical support: Q Weige, C Wa (Analytical Pharmacology); G Sukenick, H Liu, S Ruesli, H Fang (NMR Analytical Core); S Monette, SS Couto, N Pinard, J Candelier, M Jiao (Laboratory of Comparative Pathology); Molecular Cytology; Small-Animal Imaging Core Facility; S Cai, E Burnazi (Radiochemistry Core); AE Lash (Bioinformatics).

Grant Support

Charles H. Revson Senior Fellowship in Life Sciences (NJC); ASCO Young Investigator Award, AACR BMS Fellowship, K08CA140946, DOD W81XWH-10-1-0197 (YC); Department of Defense PCRP Prostate Cancer Training Award (LC); Howard Hughes Medical Institute, National Cancer Institute (5P01CA089021) (CLS); NCI Core Grant (2 P30 CA 008748-43) for partial support of the Organic Synthesis Core (OO), and 2 P50 CA092629 SPORE in Prostate Cancer.

Financial Support: Charles H Revson Senior Fellowship in Life Sciences (NJC); ASCO Young Investigator Award, AACR BMS Fellowship, K08CA140946, DOD W81XWH-10-1-0197 (YC); Department of Defense PCRP Prostate Cancer Training Award (LC); NCI Core Grant 2 P30 CA 008748-43 (OO); HHMI, NCI 5P01CA089021 (CLS), and 2 P50 CA092629 SPORE in Prostate Cancer.

References

1. Jemal A, Siegel R, Xu J, Ward E. Cancer statistics, 2010. *CA Cancer J Clin.* 2010; 60:277–300. [PubMed: 20610543]
2. Scher HI, Sawyers CL. Biology of progressive, castration-resistant prostate cancer: directed therapies targeting the androgen-receptor signaling axis. *J Clin Oncol.* 2005; 23:8253–61. [PubMed: 16278481]
3. Chen Y, Clegg NJ, Scher HI. Anti-androgens and androgen-depleting therapies in prostate cancer: new agents for an established target. *Lancet Oncol.* 2009; 10:981–91. [PubMed: 19796750]
4. Reid AH, Attard G, Danila DC, Oommen NB, Olmos D, Fong PC, et al. Significant and sustained antitumor activity in post-docetaxel, castration-resistant prostate cancer with the CYP17 inhibitor abiraterone acetate. *J Clin Oncol.* 2010; 28:1489–95. [PubMed: 20159823]
5. Danila DC, Morris MJ, de Bono JS, Ryan CJ, Denmeade SR, Smith MR, et al. Phase II multicenter study of abiraterone acetate plus prednisone therapy in patients with docetaxel-treated castration-resistant prostate cancer. *J Clin Oncol.* 2010; 28:1496–501. [PubMed: 20159814]
6. Tran C, Ouk S, Clegg NJ, Chen Y, Watson PA, Arora V, et al. Development of a second-generation antiandrogen for treatment of advanced prostate cancer. *Science.* 2009; 324:787–90. [PubMed: 19359544]
7. Scher HI, Beer TM, Higano CS, Anand A, Taplin ME, Efstathiou E, et al. Antitumour activity of MDV3100 in castration-resistant prostate cancer: a phase 1–2 study. *Lancet.* 2010; 375:1437–46. [PubMed: 20398925]
8. de Bono JS, Logothetis CJ, Molina A, Fizazi K, North S, Chu L, et al. Abiraterone and increased survival in metastatic prostate cancer. *N Engl J Med.* 2011; 364:1995–2005. [PubMed: 21612468]
9. Foster WR, Car BD, Shi H, Levesque PC, Obermeier MT, Gan J, et al. Drug safety is a barrier to the discovery and development of new androgen receptor antagonists. *Prostate.* 2010
10. Wang Q, Carroll JS, Brown M. Spatial and temporal recruitment of androgen receptor and its coactivators involves chromosomal looping and polymerase tracking. *Mol Cell.* 2005; 19:631–42. [PubMed: 16137620]
11. Wang Q, Li W, Liu XS, Carroll JS, Janne OA, Keeton EK, et al. A hierarchical network of transcription factors governs androgen receptor-dependent prostate cancer growth. *Mol Cell.* 2007; 27:380–92. [PubMed: 17679089]
12. Clegg, NJ.; Sawyers, CL. 2010. http://cbio.mskcc.org/Public/Sawyers_Clegg_ARN-509_2010/
13. Chen CD, Welsbie DS, Tran C, Baek SH, Chen R, Vessella R, et al. Molecular determinants of resistance to antiandrogen therapy. *Nat Med.* 2004; 10:33–9. [PubMed: 14702632]

14. Taplin ME, Balk SP. Androgen receptor: a key molecule in the progression of prostate cancer to hormone independence. *J Cell Biochem*. 2004; 91:483–90. [PubMed: 14755679]
15. Shidaifat F, Gharaibeh M, Bani-Ismail Z. Effect of castration on extracellular matrix remodeling and angiogenesis of the prostate gland. *Endocr J*. 2007; 54:521–9. [PubMed: 17527004]
16. Carver BS, Chapinski C, Wongvipat J, Hieronymus H, Chen Y, Chandarlapaty S, et al. Reciprocal feedback regulation of PI3K and androgen receptor signaling in PTEN-deficient prostate cancer. *Cancer Cell*. 2011; 19:575–86. [PubMed: 21575859]

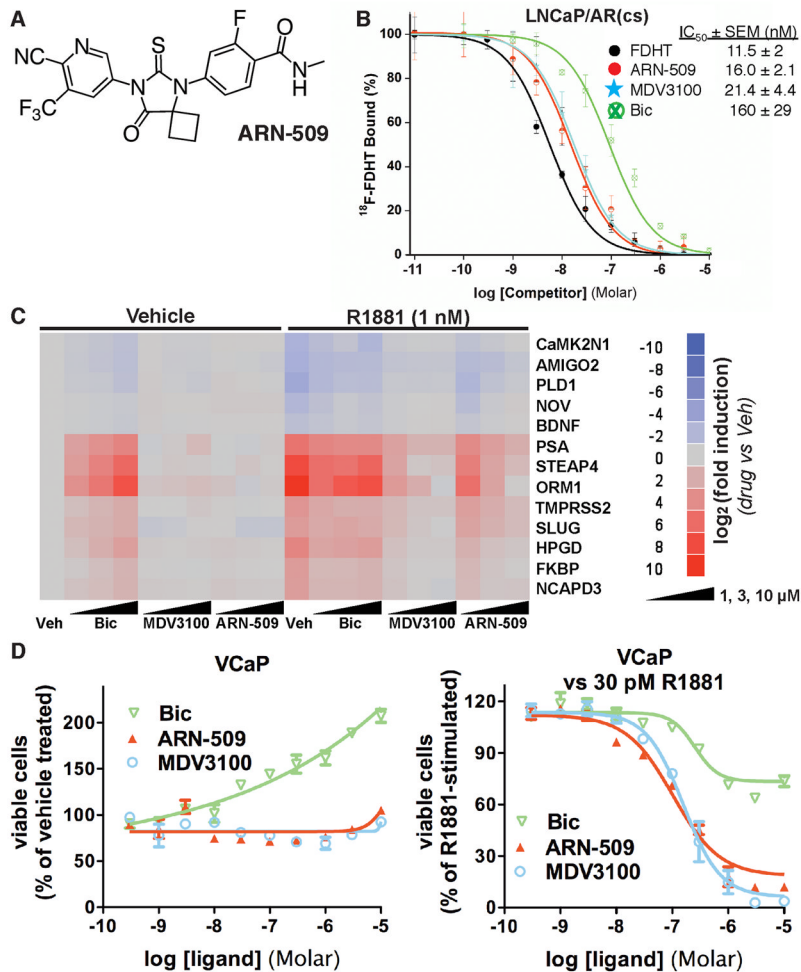
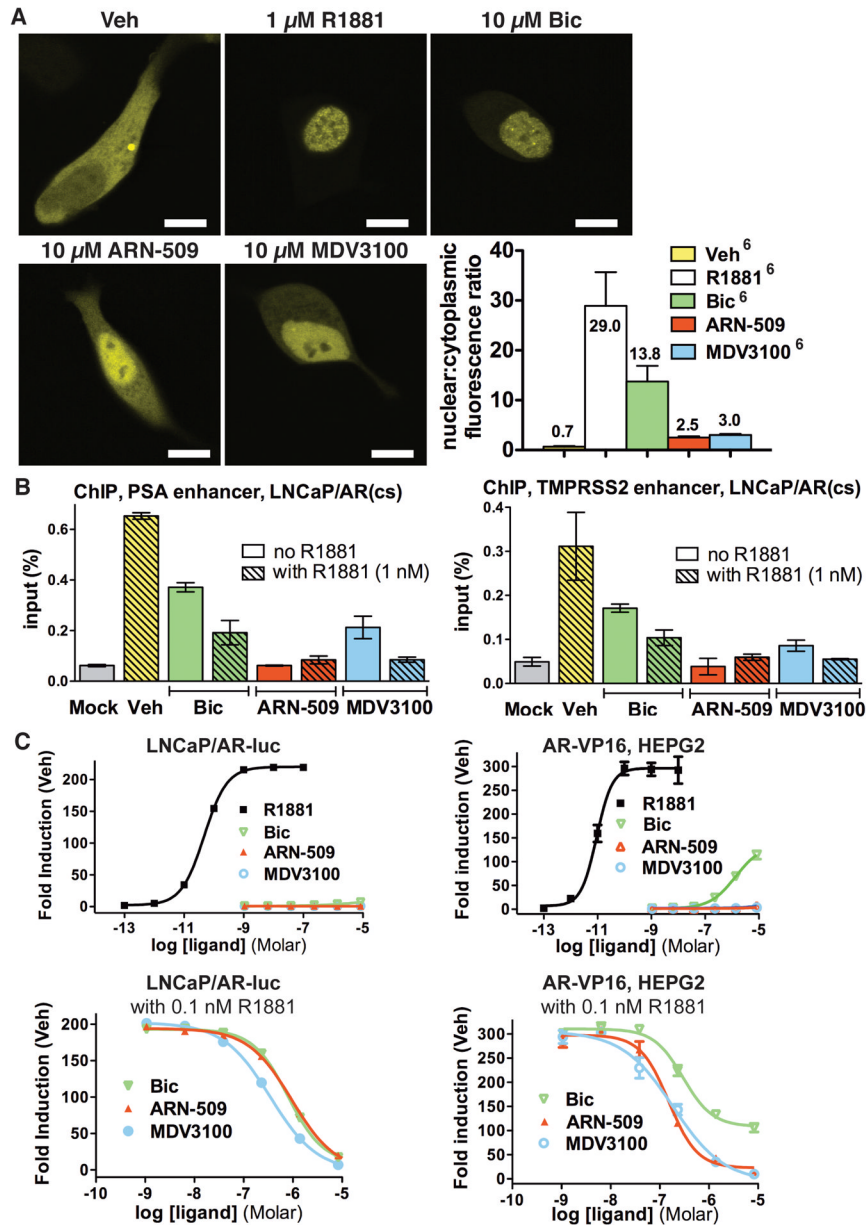


Figure 1. ARN-509 activity *in vitro* in human prostate-cancer cells

(A) ARN-509 structure. (B) Representative competitive binding-assay vs ¹⁸F-FDHT (LNCaP/AR(cs)). IC₅₀-values: 11.5nM (FDHT), 16nM (ARN-509), 21.4 nM (MDV3100), 160nM (Bic (bicalutamide)) (error-bars:SD, n=3). *Inset: IC*₅₀-values (mean ± SEM) from five replicate experiments. (C) qRT-PCR analysis of AR-regulated genes (normalized to GAPDH). LNCaP/AR(cs) cultured (5% CSS) 3d with/without 1nM R1881 and DMSO (Veh) or drug (1,3,10μM). (D) VCaP cultured (5%CSS) for 2d, then treated for 7d. *Left-panel*:agonist-mode. *Right-panel*:antagonist-mode with 30pM R1881. Viable cells (CellTiter-GLO) plotted as % vehicle-control (DMSO) (n=3, mean±SEM).

**Figure 2. ARN-509 impairs AR nuclear-localization and inhibits DNA-binding**

(A) Representative confocal microscopic images (scale-bars:10 μ m) of LNCaP with AR-EYFP cultured (5% CSS) and treated with DMSO (Veh) or drug. Nuclear:cytoplasmic fluorescence-intensity of individual cells was quantified ($n=3$, mean \pm SEM). (B) ChIP of AR in LNCaP/AR(cs) cultured (5%CSS) and treated 1h with/without 1nM R1881 and either DMSO (Veh) or 10 μ M anti-androgen. RT-PCR: PSA, TMPRSS2 enhancers (mean \pm SD, $n=2$). (C) Activation of an androgen-regulated 4XARE-Luc reporter gene by wtAR and VP16-AR in LNCaP/AR-luc or Hep-G2 cells treated for 40–48h with/without 100 pM R1881 and either DMSO (Veh), or anti-androgen. Luciferase assay conducted on cell lysates: light-units relative to vehicle-control ($n=3$, mean \pm SEM).

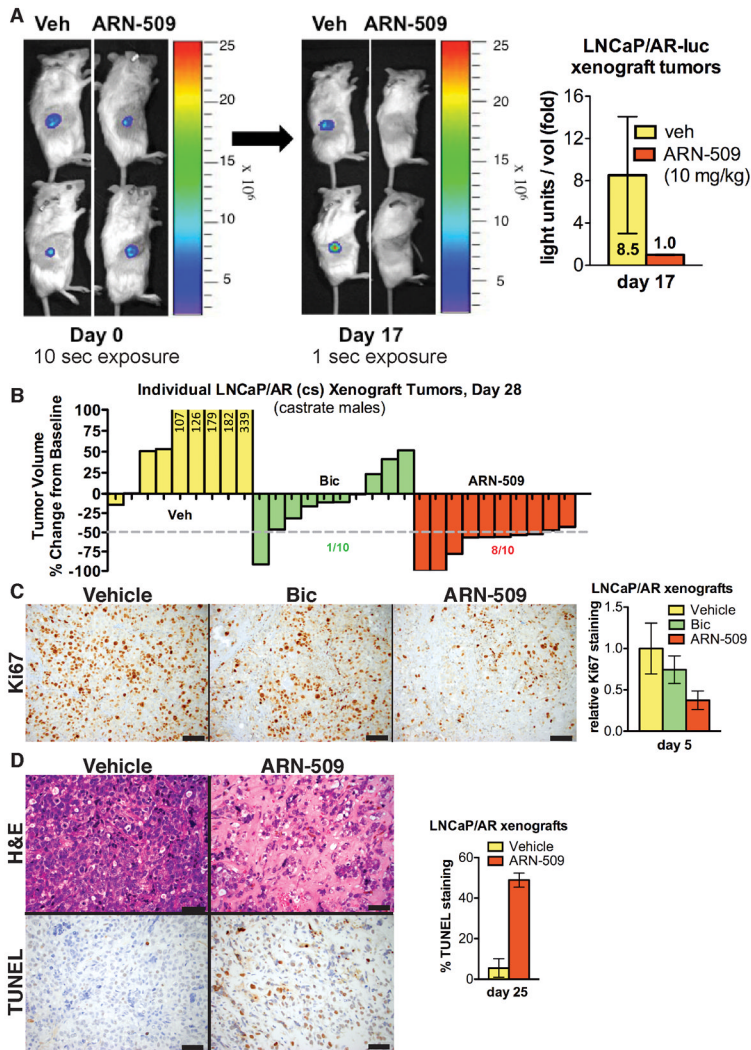


Figure 3. ARN-509 is active in models of castration-resistant prostate cancer

(A) Luciferase-imaging of castrate male mice harboring LNCaP/AR-luc tumors pre-treatment (d0) and post-treatment (d17), normalized to tumor volume. (B) Castrate male mice bearing LNCaP/AR(cs) tumors (mean tumor-volume 200mm^3) treated by daily-gavage with vehicle, or drug. % -change in individual tumor volume (9–10 tumors/treatment-group) after 28d. Unpaired t-test:Vehicle vs ARN-509: p=0.0001; Vehicle vs Bic: p=0.004; ARN-509 vs Bic: p=0.002. Plasma-concentrations measured 24h post-dose on d28 (mean $\pm\text{SEM}$: Bic 30.74 ± 3.68 ; ARN-509 9.69 ± 1.58). (C) Castrate male mice bearing LNCaP/AR tumors $>100\text{mm}^3$ treated 5d by daily-gavage with vehicle or 10 mg/kg/day anti-androgen. Ki67 IHC performed on tumor-tissue resected 2h after final dose. # positively-stained cells calculated out of 300 cells counted in each of 5 random views (n=3 tumors/treatment group), and expressed relative to vehicle-controls (error:SD; Veh vs ARN-509 and Bic vs ARN-509: p>0.05 (1-way ANOVA with Bonferroni's post-test)). (D) Castrate male mice bearing LNCaP/AR tumors treated as in (C) for 25d. TUNEL-staining performed on tumor-tissue resected after final dose. # positively-stained cells calculated, out of 300 cells counted in each of 5 random views (n=3 tumors/treatment-group), expressed relative to vehicle-controls (error:SD).

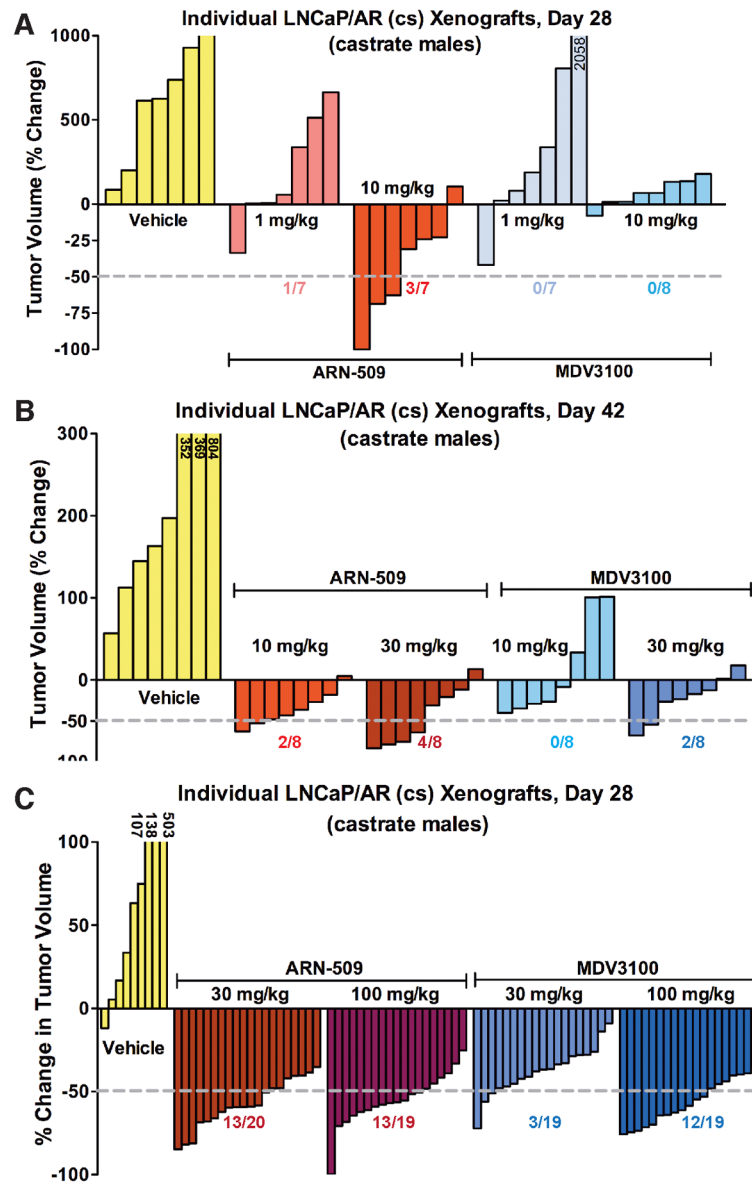


Figure 4. ARN-509 achieves similar efficacy with lower steady-state plasma-levels than MDV3100 in LNCaP/AR xenograft models of castration-resistant prostate cancer
A–C, Castrate male mice bearing LNCaP/AR(cs) tumors treated by oral daily-gavage with vehicle, ARN-509 or MDV3100. Unpaired t-test used for statistical comparisons. **(A)** 1,10 mg/kg dose: %change in individual tumor volume (n=7–8/treatment-group) after 28d-treatment. p<0.05: drug vs vehicle. **(B)** 10, 30 mg/kg dose: %change in individual tumor volume (n=8/treatment-group) after 42d-treatment. p<0.05: drug vs vehicle. **(C)** 30, 100 mg/kg dose: %change in individual tumor volume (n=19–20 tumors/treatment-group) after 28d-treatment. * p<0.05 drug vs vehicle or drug vs drug.

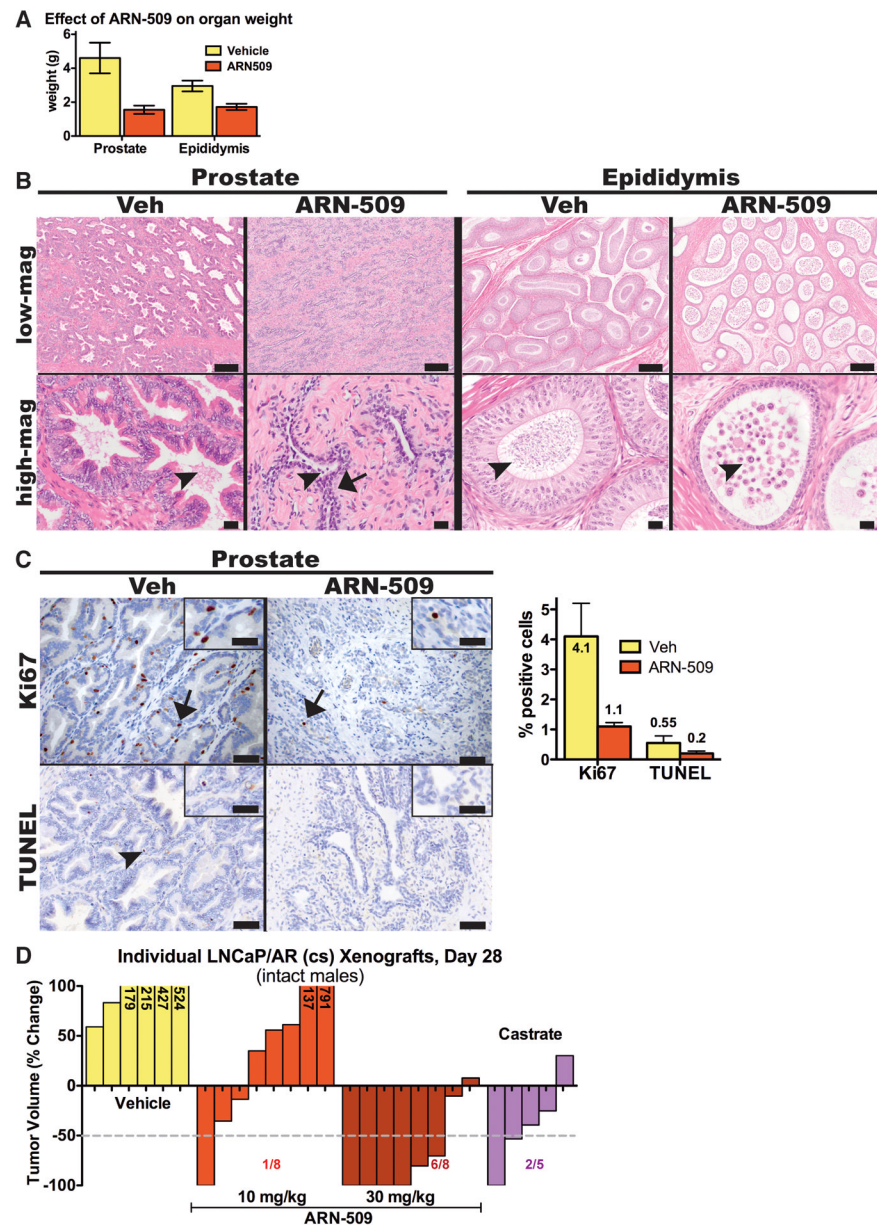


Figure 5. ARN-509 induces castrate-like changes in dog prostate and epididymis

A–C, Intact male beagle dogs treated by oral-gavage for 28d with vehicle (n=5) or ARN-509 10 mg/kg/day (n=4). Organs resected 24h after final-dose. Mean plasma-concentration of ARN-509 measured at sacrifice, 24h after final dose, was 17.5 µg/mL. (A) Prostate and epididymis weights (mean±SEM). p<0.05: Veh vs ARN-509 in prostate (2-way ANOVA, with Bonferroni post-test). Comparison for epididymis is insignificant. (B) H&E staining of transverse prostate-sections (*upper-panels*) and longitudinal epididymis sections (*lower-panels*) at low-power (100x, scale bar:200µm) and high-power (600x, scale-bar:20µm). *Upper-panels*: Fully-mature, active acini in vehicle-treated prostate containing intraluminal secretions (*arrowhead*), lined with folds of a single-layer of columnar epithelial cells with abundant cytoplasm. ARN-509-treated prostates: bilayer of cuboidal epithelial cells (*arrow*), small lumens with rare eosinophilic secretory material (*arrowhead*). *Lower-panels*: Vehicle-treated epididymis: tall columnar pseudo-stratified epithelium with lumens containing

abundant spermatozoa (*arrowhead*). ARN-509-treated epididymis: cuboidal epithelium, lumens with little-to-no spermatozoa, containing multi-nucleated round cells suggestive of sloughed degenerate germ cells (*arrowhead*). (C) Dog prostates stained with antibody to Ki67 (200x, scale-bar:100 μ m) or TUNEL (400x, scale-bar:50 μ m). Ki67-staining (*arrows*) and TUNEL (*arrowheads*). No TUNEL-staining is evident in ARN-509-treated prostates. Results quantified as mean percentage (\pm SEM) of positive cells from representative areas from each prostate (n=5 for vehicle, n=4 for ARN-509). p<0.05 for TUNEL staining of Veh vs ARN-509 (1-way ANOVA with Bonferroni's multiple comparison post-test). (D) Intact male mice bearing LNCaP/AR(cs) tumors, treated for 28d by oral daily-gavage with vehicle, ARN-509 or MDV3100 (10, 30 mg/kg). %change in individual tumor volume (n=5–8/treatment-group) after 28d-treatment.. * p<0.05 for each treatment relative to vehicle (unpaired t-test).

Table 1**ARN-509 and MDV3100 steady-state levels in plasma and in LNCap/AR(cs) xenograft tumor-tissue after 28d dosing**

After 28d of dosing at 1 and 10 mg/kg/day, plasma and tumor-tissue concentrations of ARN-509 and MDV3100 were quantified 24h after final drug-dose using an LC/MS/MS method.

Dose (mg/kg/day)	# mice	^a Plasma C _{24hr} (µg/mL)	^a Tumor C _{24hr} (µg/g)	Tumor:Plasma Ratio (%)
ARN-509	1	0.425 ± 0.16	0.991 ± 0.30	259 ± 11
	10	3.31 ± 0.98	3.26 ± 0.82	107 ± 44
MDV3100	1	1.08 ± 0.26	0.439 ± 0.12	45.1 ± 24.8
	10	11.0 ± 2.5	3.39 ± 1.50	30.5 ± 12.8

^a mean ± SD

Table 2
ARN-509 and MDV3100 steady-state levels in plasma- and brain-tissue

ARN-509 and MDV3100 were measured in plasma- or brain-tissue following 28d daily-dosing at 10 mg/kg/day. Plasma and brain were isolated 24h after final-dose on d28. ARN-509 and MDV3100 levels quantified using an LC/MS method.

Dose (mg/kg/day)	# mice	^a Plasma C _{24hr} (µg/mL)	^a Brain C _{24hr} (µg/g)	Brain:Plasma (%)
ARN-509	10	8	1.64 ± 0.30	0.479 ± 0.132
MDV3100	10	5	10.5 ± 2.3	2.01 ± 0.83

^a mean